Experimental and Theoretical Study of Salt-Dome Evolution

Hans Ramberg
Institute of Geology
University of Uppsala
Uppsala, Sweden

ABSTRACT

As a part of a program of experimental and theoretical research in the field of tectonics at the Institute of Geology, University of Uppsala, the evolution of salt-dome structures has been studied. The chief experimental study has been performed by means of more or less realistically scaled models run in a large-capacity centrifuge in which the centrifugal force imitates the force of gravity. A large number of realistically looking dome-type structures have thus been produced in layered models in which rather stiff materials simulate rock strata. Coherent flow as well as cataclastic processes occur during the runs thus giving the models a natural appearance.

Application of scale-model theory permits one to calculate the time of evolution of natural-sized domes on basis of the small centrifuged models.

Complementary to the experimental work fluid-dynamic theory has been applied to the domal process. Theory and experiments show in general consistent results.

Salt tectonics, particularily the evolution of salt domes, should be studied with deep interest by all earth scientists concerned with the tectonic development of the earth's crust and mantle. The relatively high mobility of saline deposits makes the tectonic evolution of salt-bearing complexes serve as a striking model for the behavior of the less mobile but yet often strongly deformed silicate rocks. A knowledge of deformation structures in saline deposits makes it easier for hard-rock geologists to accept the condition that the complicated structural pattern encountered in gneisses and crystalline schists, for example, also has developed by flowage in the crystalline state. Without the experience gained from the study of salt domes, our view on the common granitic and gneissic domes and anticlinal cores would probably have been that such bodies were emplaced in the liquid state. It would have appeared especially unacceptable to many (it still does to some!) that buoyant forces generated by but small density differences were responsible for the rise of the crystalline masses. It is now well established both experimentally (e.g. Nettleton, 1943; Parker and McDowall, 1955; and many others) and theoretically (Arrhenius, 1912; Daneš, 1964; Biot *et al.*, 1965; Ramberg, 1967, 1968) that the primary reason for the rise of salt domes is the buoyant force of a light layer of salt overlain by more dense sediments. There is, however, room for considerable improvement both of the theory and the experimental technique.

THEORETICAL APPROACH

To treat dome evolution theoretically the complexity of natural structures must be reduced quite drastically without, however, losing the essential features, namely that the original structures were stratified with horizontal layering and that the densities were inverted. If we furthermore assume that the salt and the overburden behave as viscous media, albeit with very high viscosity, fluid-dynamic theory yields considerable information on the evolution of the domal structures.

As the mathematics of the theory, which is quite involved, is presented in detail in other papers (Daneš, op. cit.; Biot *et al.*, op. cit.; Ramberg, op. cit. and paper in press) let it here suffice to

emphasize the essential conclusions. The theory shows that the salt layer (or any other buoyant layer) tends to develop sinusoidal waves with a randomly distributed wavelength while the amplitude still is very small. The wavy perturbations grow with different rates, and it appears that, in any given system, perturbations with a certain wavelength grow faster than both longer and shorter waves. As the rate of rise is proportional to the amplitude (as long as the waves are gentle) the perturbations which show maximum rate of growth soon dominate completely the development of the structure. Hence the wavelength of the dominant wave determines the spacing between the domes or ridges which rise spontaneously from a layer of salt.

The ratio between the wavelength of the dominant perturbation and the thickness of the salt layer depends upon several dimensionless parameters of the systems, viz. (1) the viscosity ratio between overburden and salt, μ_1/μ_2, (2) the viscosity ratio between salt and substratum, μ_2/μ_3, (3) the ratio between the thicknesses of the overburden and of the salt layer, h_1/h_2, (4) the ratio of the thicknesses of the salt and of its substratum, h_2/h_3, (5) the ratio between the density of the overburden and the density difference between the overburden and the salt, $\rho_1/(\rho_1-\rho_2)$, and finally (6) the ratio between the density contrasts between the overburden and the salt and between the salt and the substratum, $(\rho_1-\rho_2)/(\rho_2-\rho_3)$.

The effect of each of these six dimensionless parameters which characterize the dynamics of the complex is generally as follows (We assume that the parameter noted in each of the points below varies while the five others are kept constant.): The wavelength/thickness ratio for the dominant fast-growing perturbation increases when; (1) μ_1/μ_2 increases, (2) μ_2/μ_3 increases, (3) h_1/h_2 increases (up to a certain limit), (4) h_3/h_2 increases (also up to a certain limit), (5) $\rho_1/(\rho_1-\rho_2)$ decreases, and finally (6) $(\rho_1-\rho_2)/(\rho_2-\rho_3)$ increases.

In the special case in which the overburden is thicker than the dominant wavelength and the salt stratum rests on a rigid substratum, the only parameter that controls the wavelength-thickness ratio, and hence the spacing between the domes (in this idealized theory), is the parameter μ_1/μ_2. The density contrast also in this case, of course, controls the rate of rise but not the spacing between the ascending bulges. Figure 1 shows the function $v/yq = f(\lambda/h)$ at selected viscosity ratios between salt and overburden. The rate of growth of amplitude is v and y is aplitude while λ is wavelength and h the thickness of the salt layer. q is defined in equation (1) below. The ratio v/y, which we have called the rate of relative amplitude growth, is an important quantity in the perturbation theory of domal evolution.

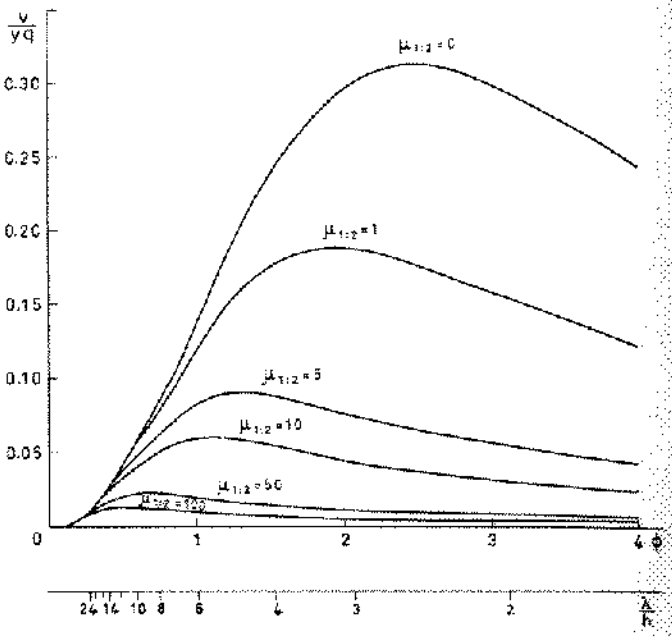

Figure 1. Rate of relative amplitude growth, v/yq, as a function of wavelength/thickness ratio of buoyant layer below overburden of infinite thickness. $\mu_{1:2}$ is viscosity ratio between overburden and "salt" layer.

In a more general model the salt rests upon a mobile substratum and the overburden is thinner than the dominant wavelength such that the deformation of the buoyant salt layer penetrates up to the free surface as it were, and throws into a wavy pattern as indicated on Figure 2. The wavelength of the dominant perturbation is now depending upon all the parameters μ_1/μ_2, μ_2/μ_3, h_1/h_2, h_2/h_3, $\rho_1/(\rho_1-\rho_2)$ and $(\rho_1-\rho_2)/(\rho_2-\rho_3)$ of the system. As numerical examples we show in Table I how variations in μ_1/μ_2, μ_2/μ_3 and h_1/h_2 effects the dominant wavelength. In all cases shown the ratio $\rho_1/(\rho_1-\rho_2) = 10$, and $(\rho_1-\rho_2)/(\rho_2-\rho_3) = -1$. The data are based on a mathematical model presented in Ramberg (1968).

EXPERIMENTAL STUDY

Theoretical study alone cannot fully explain the details of domal evolution in complicated natural

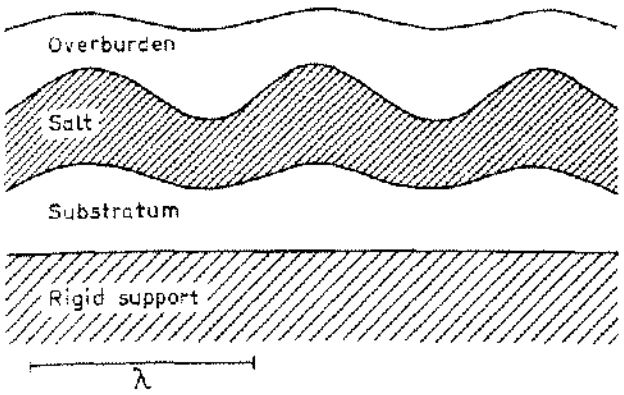

Figure 2. Salt stratum resting on mobile substratum and rising through overburden of limited thickness (See Table 1).

systems with irregular geometry and nonlinear rheological properties of the rocks. An experimental approach is needed by means of which the mechanism of evolution can be studied in great detail. Though experimentation has been performed probably more extensively in salt tectonics than in any other field of structural geology, the technique employed has not permitted study of much of the detail which characterizes salt-dome structures (Nettleton, 1943; *et al.*, 1947; Parker *et al.*, 1955). The limitation relates to the scale-model theory pertaining to gravity-driven dynamic processes. As has been known since the time of Galileo and emphasized especially relative to geotectonic processes by Hubbert (1937), in order for laboratory models of manageable size to simulate realistic geotectonic processes driven by gravity, the model materials must be fluids such as ordinary liquids and mechanically as weak as loose powder. It is very difficult to study complicated three-dimensional structures in such materials. The structures will sag and deform under their own weight prematurely while the models are being constructed, not to speak of the disturbances which will occur during the inspection of the results, a procedure which often requires sectioning of the three-dimensional models. In view of the difficulties of this nature, it is surprising that methods which increase the body force, for example, by employing centrifugal force have not been utilized until quite recently in experimental tectonics. Such methods permit one to utilize mechanically stronger model materials without violating the laws of dynamic similarity. It is thus possible to use plastic and viscoelastic solids rather than liquids to simulate the rocks in the models. The choice of available materials increases greatly such that model materials with the proper combination of rheological properties and density are more readily obtained. The construction of the models can be done at ease, eliminating disturbing premature sagging prior to exposing the models to the increased body force. Study of the resulting structures can likewise be performed without the danger of damage by sagging after the runs are finished. In short, it is possible to make the dynamic models more quantitative and more realistic.

Table 1. Dominant Wavelength in Relation to Viscosities and Thicknesses of Triple Layer Models.

$\rho_1/(\rho_1-\rho_2) = 10$, $(\rho_1-\rho_2)/(\rho_2-\rho_3) = -1$, $h_2/h_3 = 1$.

μ_1/μ_2	μ_2/μ_3	h_1/h_2	$\frac{\lambda max}{h_2}$
100	100	1	6.98
100	0.01	1	5.71
1	100	1	4.83
1	0.01	1	3.48
100	100	0.5	8.49
100	0.01	0.5	7.65
1	100	0.5	6.15
1	0.01	0.5	4.62
100	100	0.1	12.31
100	0.01	0.1	12.31
1	100	0.1	7.50
1	0.01	0.1	7.56

To increase the body force the writer and his co-workers are employing centrifuges, the largest of which takes models weighing up to 10 kg and measuring 20 cm in diameter. The maximum centripetal acceleration is 4,000 times the acceleration due to gravity. Materials strong enough for easy handling and construction of the models can be used without violating the scale-model laws because of the augmented body-force field.

As the laboratory equipment and the model material have been described elsewhere (e.g. Ramberg (1967), let it suffice here to reproduce a sketch of the instrument (Fig. 3) and to list the properties of the model materials.

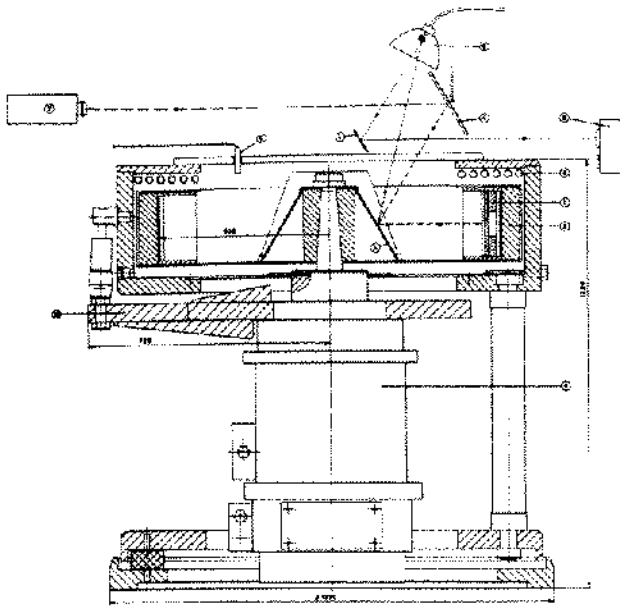

Figure 3. Cross section through the new centrifuge in the tectonic laboratory in Uppsala. 1: model placed in the rotor, 2: rotor, 3: cooling tubes, 4: mirrors, 5: stroboscope lamp, 6: trigger for stroboscope, 7: camera, 8: taxometer, 9: motor, 10: flexible support. Dimensions given in millimeters.

The importance of the increased acceleration is best seen when the theory of dome evolution mentioned above is adjusted to a body-force field whose acceleration coefficient is different from that of the earth's gravitational field. The rate of amplitude growth of the perturbations in a given layered model in the earth's gravitational field is controlled by relationships of the following type,

$$(1)\quad \frac{\partial \gamma}{\partial t} = k\,\frac{(\rho_i - \rho_{(i+1)})h_{(i+1)}g}{2\mu_{(i+1)}}\gamma \equiv kq\gamma$$

where k is a constant characterizing the system, ρ_i-$\rho_{(i+1)}$ is the density contrast between two selected layers i and $(i+1)$, $h_{(i+1)}$ the thickness and $\mu_{(i+1)}$ the viscosity of layers $(i+1)$. The acceleration due to gravity is g. If the same model is exposed to the centrifugal force in a centrifuge the rate of amplitude growth is governed by the same equation with the important exception however, that g is now replaced by the centripetal acceleration, a (though with opposite sign).

Thus since a is up to 4,000 g in our present set-up it follows that the rate of growth of the domes in the centrifuged model is 4,000 times faster than in the non-centrifuged model. Or, what is more important, it means that model materials which are up to 4,000 times stronger or show a viscosity 4,000 times higher can be employed without increasing the experimental times relative to identical non-centrifuged models. Figures 4, 5, and 6 show some non-centrifuged models consisting of materials fluid enough to evolve without the use of a centrifugal force. Figures 7 to 23 all show centrifuged models containing materials too stiff or too strong to permit domal evolution without utilization of the centrifuge.

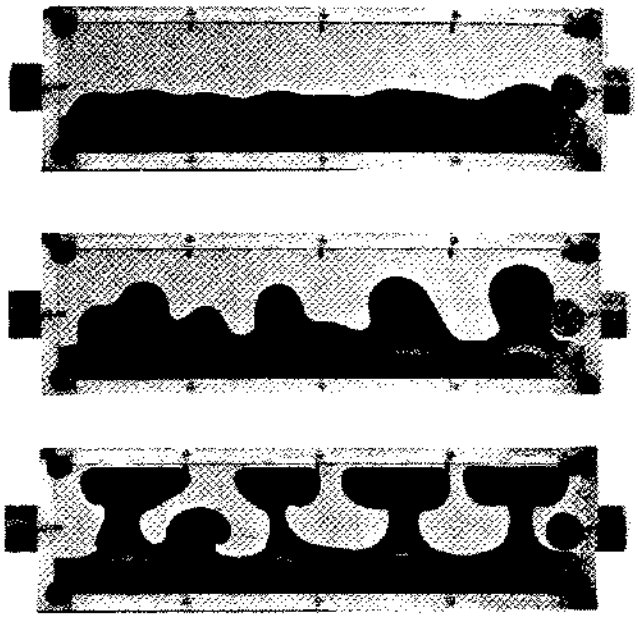

Figure 4. Layer of oil rising through overburden of syrup shown in three stages. The boundary between the two media was originally straight and horizontal. Spacing between domes (the wavelength) is always the same in repeated experiments with same substances. See theoretical discussion and Figure 1. Length of container 35 cm. Non-centrifuged model.

EXAMPLES OF SCALE-MODEL CALCULATION OF RATE OF RISE OF DOME

The somewhat uncontrollable rheological characteristics of the painter's putty and the modeling clay used as overburden in dome models are not a very good basis for quantitative scale-model calculations. Nevertheless, we provide an example of how the rate of rise of a natural domal structure

Table 2.
Model Materials Used.

Type of material	Density, g/cm³	Viscosity, poises
Modeling clay	1.6 - 1.7	$5 \cdot 10^7 - 8 \cdot 10^8$
Painter's putty	1.80 - 2.18	$\geqq 10^5$
Silicone putty, pure	1.12	$\sim 2 \cdot 10^5$
Silicone putty-magnetite or tungspar powder mixtures	1.2 - 2.1	$5 \cdot 10^5 - 2 \cdot 10^6$
Collophony-ethyl phthalate mixtures	~1	$10^6 - 10^8$

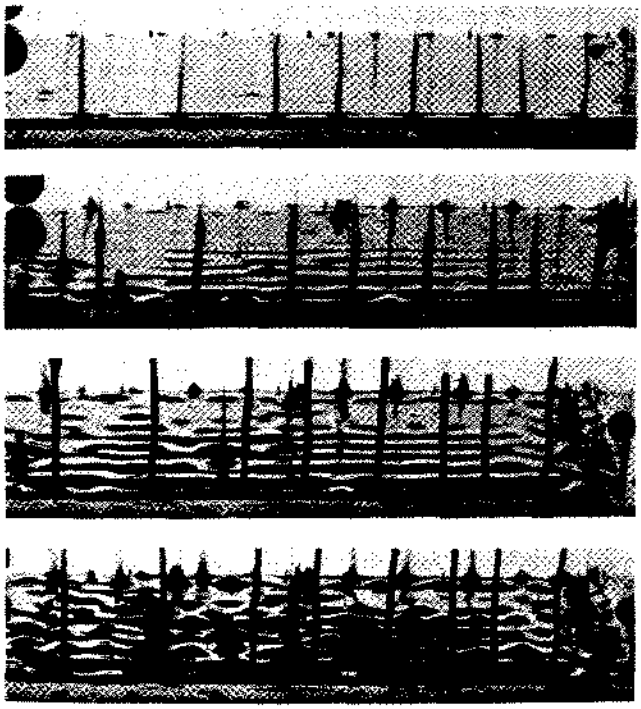

Figure 5. Layer of oil (black) rising through liquid overburden (aqueous solution); shown in four stages. Note anticlines parallel to edge of container, and domes formed on anticlines in stage four (bottom figure). Non-centrifuged model.

may be estimated from an experimental dynamic model. Model S216 (Fig. 24) is very suitable.

Significant geometric dimensions and physical properties of the model are listed in Table 3, which

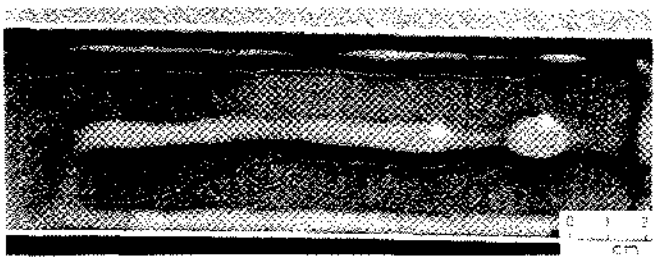

Figure 6. Anticline of silicone putty rising from originally flat and straight layer through overburden of syrup. Note orientation of anticline in relation to shape of container. Non-centrifuged model.

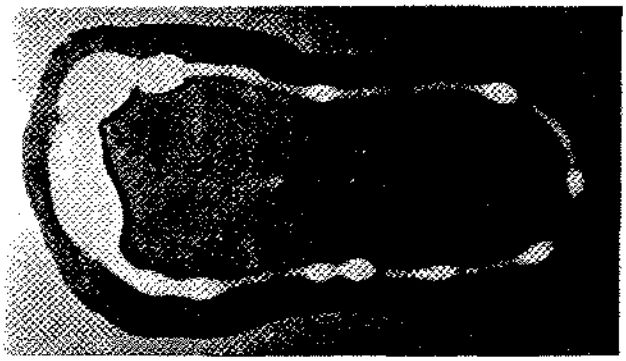

Figure 7. Anticline rising along irregular edge of layer of silicone putty overlain by syrup. Non-centrifuged model.

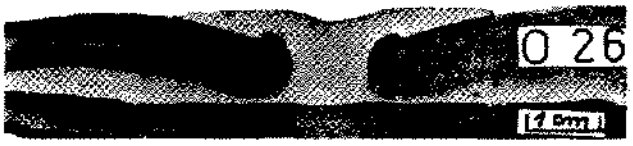

Figure 8. Cross section through centrifuged model of silicone dome having penetrated overburden of painter's putty. Note marginal sinks and spreading of 'hat' on free surface.

also gives the dimensions of a similar natural dome of salt and reasonable physical properties of the constituent rocks. Model ratios of the various properties are also given.

We wish to find the time needed for the evolution of a natural salt dome dynamically similar to the model. To find the rate of rise of the natural dome, it is necessary to know the time required for evolution of the model dome and the centripetal acceleration to which the model was subjected.

Now, since the centrifuge needs some time to attain a given angular velocity, the model was not subjected to a constant acceleration throughout the run, which lasted 26 min 25 sec. As a matter of fact, it took 3 min 45 sec to raise the velocity to the 2,200 rpm (= 1,520 g) at which the model was run for 18 min 15 sec. The velocity was then increased rapidly to 2,800 rpm (= 2,500 g) and maintained at this level for 4 min 35 sec, until the run was stopped.

Because of the low average acceleration during the relatively short period of time before the 2,200 rpm level was reached, we do not introduce a large error by disregarding, for the sake of convenience, the first 3 min 45 sec in our calculations (After all, lack of exact knowledge of the physical properties

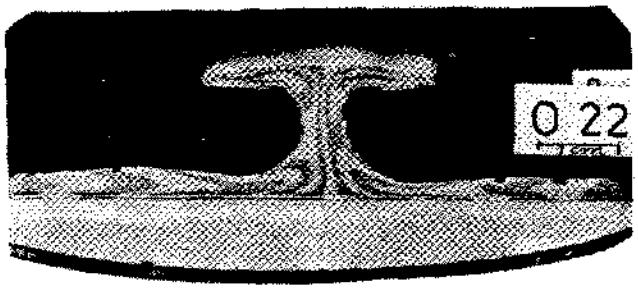

Figure 9. Flow pattern in centrifuged silicone dome in painter's putty. Marker consisted originally of bars of silicone with contrasted color having rectangular cross sections and oriented normal to the dome profile shown.

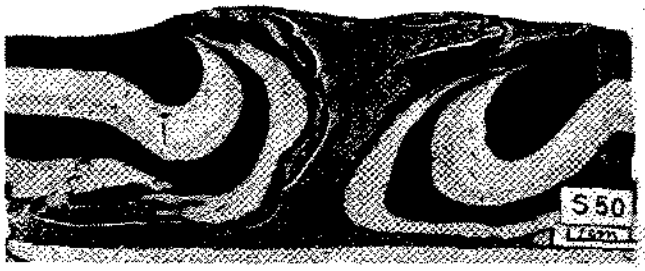

Figure 10. Deformed layered overburden of multicolored painter's putty adjacent to silicone dome formed from originally straight layers. Note boudinage of originally continuous and straight sheet of modelling clay embedded in the buoyant silicone layer. Centrifuged model.

Table 3. Example of Scale-Model Calculation of Time of Rise of Salt Dome.

Quantity	Model S216	Natural salt dome	Model ratios
Thickness of buoyant layer	5 mm	500 m	$l_r = 10^{-5}$
Total thickness of overburden	20 mm	2000 m	$l_r = 10^{-5}$
Thickness of each competent layer	1 mm	100 m	$l_r = 10^{-5}$
Thickness of incompetent layer directly above source	5 mm	500 m	$l_r = 10^{-5}$
Thickness of each incompetent layer	2 mm	200 m	$l_r = 10^{-5}$
Diameter of dome	Variable (Fig. 78)	Variable	
Density of buoyant material	1·48 g/cm³	2·22 g/cm³	$\rho_r = 0{\cdot}67$
Density of competent overburden	1·72 g/cm³	2·55 g/cm³	$\rho_r = 0{\cdot}67$
Density of incompetent overburden	1·80 g/cm³	2·70 g/cm³	$\rho_r = 0{\cdot}67$
Viscosity of buoyant layer	5.10^5 poises	10^{18} poises	$\mu_r = 5.10^{-13}$
Viscosity of incompetent overburden	10^6–10^7 poises	2.10^{11}–2.10^{19} poises	$\mu_r = 5.10^{-13}$
Viscosity of competent overburden	3.10^8 poises	6.10^{20} poises	$\mu_r = 5.10^{-13}$
Body force per unit mass, first period	1520 g cm/sec²	1 g cm/sec²	$a'_r = 1520$
Body force per unit mass, second period	2500 g cm/sec²	1 g cm/sec²	$a''_r = 2500$
Stress, first period	Variable	Variable	$\sigma'_r = \rho_r l_r a'_r = 10{\cdot}2.10^{-3}$
Stress, second period	Variable	Variable	$\sigma''_r = \rho_r l_r a''_r = 1{\cdot}68.10^{-3}$
Time, first period	1095 sec	t'_o	$t'_r = \mu_r \sigma_r^{-1} \approx 5.10^{-11}$
Time, second period	275 sec	t''_o	$t''_r = \mu_r \sigma_r^{-1} \approx 3.10^{-11}$
Total time of rise	1370 sec	t_n	

$t'_o = t'_m/t'_r = 1095/5.10^{-11} = 2{\cdot}19.10^{13}$ sec
$t''_o = t''_m/t''_r = 275/3.10^{-11} = 0{\cdot}92.10^{13}$ sec
Total time of rise: $3{\cdot}11.10^{13}$ sec $\approx 10^6$ years

Figure 11. Centrifuged model of silicone dome (black central body) having deformed a layered overburden consisting of alternating modelling clay and painter's putty.

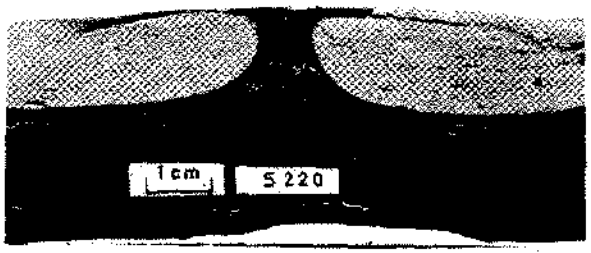

Figure 12. Model of uplifted heavy basement (black) below a silicone dome having risen through painter's-putty overburden during centrifugation. Note also boudins formed of a sheet of modelling clay embedded in the buoyant layer that ascended as dome.

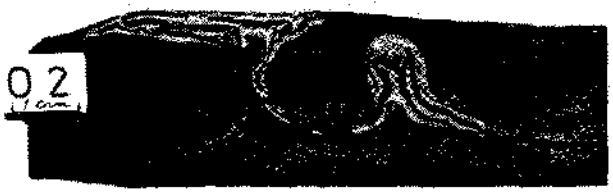

Figure 13. Silicone domes with two inlayers of modelling clay having ascended from buoyant horizontal layer embedded in painter's putty. Note the "sucking" up of the basement into the trunk of the domes.

Figure 14. Centrifuged model showing intense folding generated in surficial strata when being sucked down in the rim synclines adjacent to a rising dome.

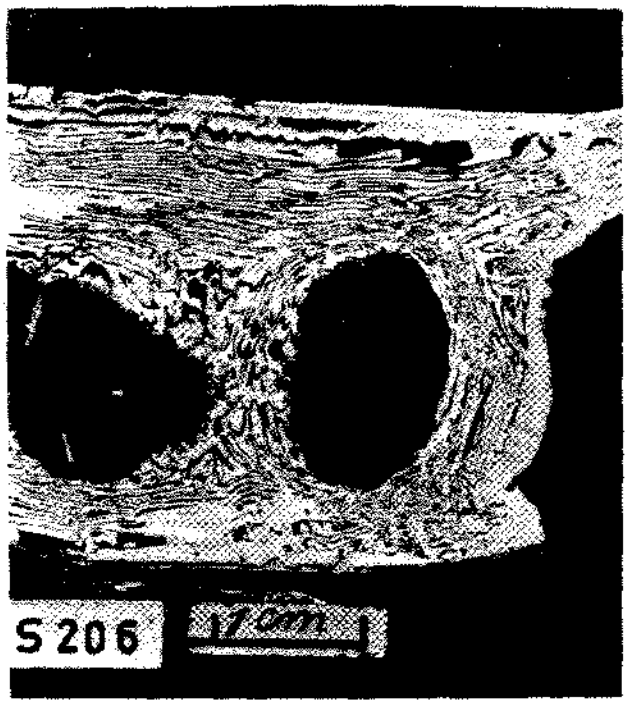

Figure 15. Same model as shown in Figure 14, but viewed from above after a surface layer has been cut off to show the folding of the strata.

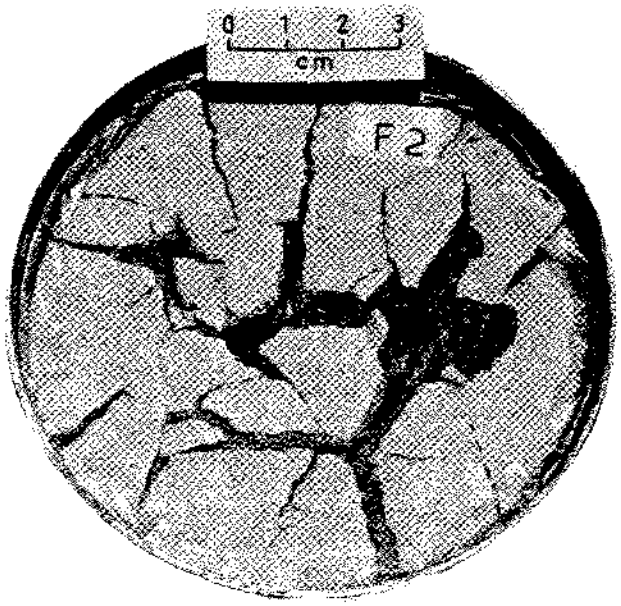

Figure 16. Domes of stitching wax (collophony-ethyl phthalate mixture) creating fractures when penetrating a surface sheet of concrete.

Figure 17. Cross section of folds and domes generated during centrifugation of stratified model with inverted density stratification. Density of the silicone strata with contrasted color increased step wise upward prior to run.

Figure 18. Model with overburden removed to show buckling of embedded sheet of modelling clay as generated while the buoyant silicone stratum developed into a central dome. The dome is cut horizontally close to its "root."

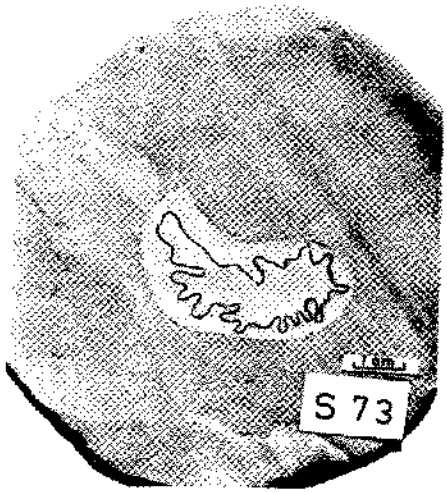

Figure 19. Same model as shown in Figure 18 shown in a horizontal section cut close to the surface of the overburden. Note buckling of embedded modelling clay sheet.

Figure 20. Cross section of silicone domes with strongly folded sheets of modelling clay.

Figure 21. Cross section of centrifuged model with three irregular domes of silicone (dotted) having ascended from a buoyant layer through overburden of interlayered painter's putty and modelling clay. The uppermost light-colored strata consist of silicone and modelling clay.

Figure 22. Same model as in Figure 21, but now shown from above. Note fracture pattern above the three elongate domes.

of the rocks would introduce much larger error.). The model is therefore regarded as being subjected to only two periods of acceleration, viz. 1095 sec at 1,520 g and 275 sec at 2,500 g.

Because of the dissimilar accelerations the two periods have different ratios of time, as given in Table 3.

The period of 1095 sec in the model evolution gives the following time for development of the natural structure:

$$t'_0 = t'_m t'^{-1}_r = 1095\ \text{sec} \cdot \frac{1}{5} \cdot 10^{11} = 2.19 \cdot 10^{13}.$$

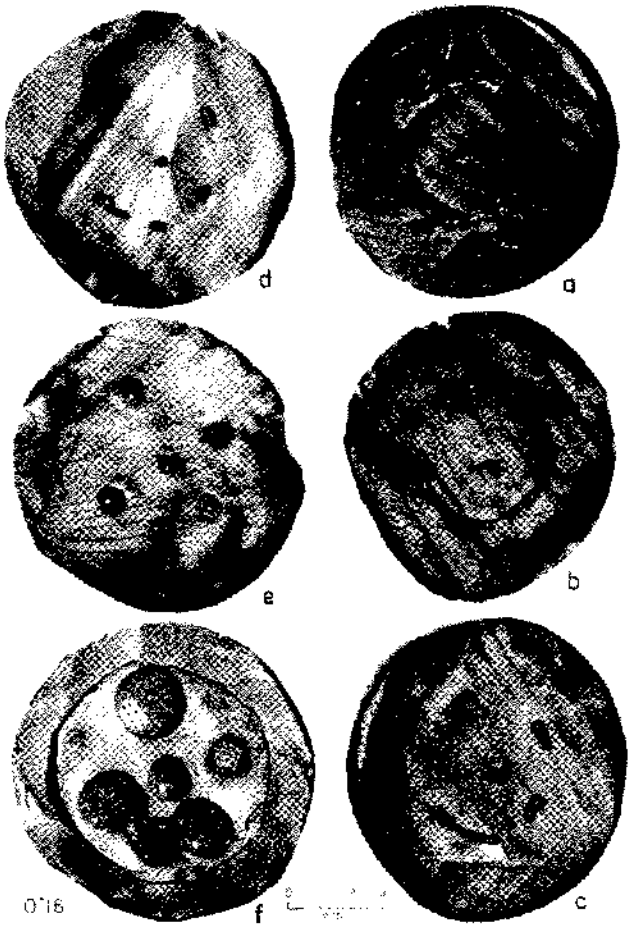

Figure 23. Horizontal sections at unlike depths through model of silicone anticline and domes (dotted) rising through overburden of painter's putty. Deepest section (just above the source layer of the domes) is a, f is free surface.

Figure 24. Model described in Table 2.

The second period of 275 sec in model evolution corresponds to

$$t''_{0\,m\,r} = t''\,t'^{-1} = 275\ \text{sec} \cdot \frac{1}{3} \cdot 10^{13} = 0.92 \cdot 10^{13}\ \text{sec}$$

for the natural structure.

Our result is then that a natural structure whose dimensions and constituent rocks are as given in Table 3 needs about 10^6 years to evolve to the same stage as the model has evolved. This is quite a reasonable result.

ACKNOWLEDGMENT

This work has been supported by grants from the Swedish Natural Science Research Council (2392-24) and the Swedish Board for Technical Development (69-283/U181).

REFERENCES

Arrhenius, S., 1912, Zur Physik der Salzlagerstätten: Meddelanden från K. Vetenskapsakademiens Nobelinstitut, v. 2, no. 20.

——, and Lachmann, R., 1912, Die phys.-chem. Bedingungen bei den Bildungen der Salzlager und ihre Anwendungen auf geologische Probleme: Geol. Rundschau, v. 3, p. 139.

Biot, M.A., and Odé, H., 1965, Theory of gravity instability with variable overburden and compaction: Geophysics, v. 30, p. 213.

Cater, F.W., and Elston, D.P., 1963, Structural development of salt anticlines of Colorado and Utah: Am. Assoc. Petroleum Geologists Mem. 2, p. 152.

Daneš, Z.F., 1964, Mathematical formulation of salt-dome dynamics: Geophysics, v. 29, p. 414.

Escher, B.G., and Kuenen, P.H., 1929, Experiments in connection with salt domes: Leidse Geol. Mededel., v. 3, p. 151.

Hubbert, M.K., 1937, Theory of scale models as applied to the study of geologic structures: Geol. Soc. America Bull., v. 48, p. 1459.

Nettleton, L.L., 1934, Fluid mechanics of salt domes: Am. Assoc. Petroleum Geologists Bull., v. 17, p. 1175.

——, 1943, Recent experimental and geophysical evidence of mechanics of salt-dome formation: Am. Assoc. Petroleum Geologists Bull., v. 27, p. 51.

——, 1955, History of concepts of Gulf Coast salt-dome formation: Am. Assoc. Petroleum Geologists Bull., v. 39, p. 2373.

——, and Elkins, T.A., 1947, Geologic models made from granular materials: Am. Geophys. Union Trans., v. 28, p. 451.

Parker, T.J., and McDowell, A.N., 1955, Model studies of salt-dome tectonics: Am. Assoc. Petroleum Geologists Bull., v. 39, p. 2384.

Ramberg, H., 1963, Experimental study of gravity tectonics by means of centrifuged models: Geol. Inst. Univ. Uppsala Bull. 42, p. 1.

———, 1967, Gravity, deformation and the earth's crust: London and New York, Academic Press, 214 p.

———, 1968, Instability of layered systems in the field of gravity I and II: Phys. Earth Planet. Interiors, v. 1, p. 427.

von Trusheim, f., 1957, Ueber Halokinese und ihre Bedeutung für die strukturelle Entwicklung Norddeutschland: Z. Deut. Geol. Ges., v. 109, p. 111.

———, 1966, Mechanism of salt migration in northern Germany: Am. Assoc. Petroleum Geologists Bull., v. 44, p. 1579.